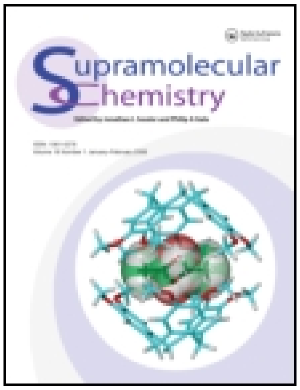

Supramolecular Chemistry
Publication details, including instructions for authors and subscription information:
http://www.tandfonline.com/loi/gsch20

Self-assembly and nanostructure formation of amphiphilic 4,5-bis(2-pyridylethynyl)tetrathiafulvalenes

Eigo Isomura [a] , Tohru Nishinaga [a] & Masahiko Iyoda [a]
[a] Department of Chemistry, Graduate School of Science and Engineering, Tokyo Metropolitan University, Hachioji, Tokyo, 192-0397, Japan

To cite this article: Eigo Isomura, Tohru Nishinaga & Masahiko Iyoda (2011): Self-assembly and nanostructure formation of amphiphilic 4,5-bis(2-pyridylethynyl)tetrathiafulvalenes, Supramolecular Chemistry, 23:03-04, 304-309

To link to this article: http://dx.doi.org/10.1080/10610278.2010.527978

Supramolecular Chemistry
Vol. 23, Nos. 3–4, March–April 2011, 304–309

Self-assembly and nanostructure formation of amphiphilic 4,5-bis(2-pyridylethynyl)tetrathiafulvalenes

Eigo Isomura, Tohru Nishinaga and Masahiko Iyoda*

Department of Chemistry, Graduate School of Science and Engineering, Tokyo Metropolitan University, Hachioji, Tokyo 192-0397, Japan

(*Received 9 July 2010; final version received 3 September 2010*)

Amphiphilic tetrathiafulvalene (TTF) having both long alkylthio chains and pyridylethynyl groups was synthesised, and its nanostructure and redox properties were investigated. The bis(pyridylethynyl)TTF formed 1D flat and helical tapes. Since these tapes were of micrometre size, the conductivities of neutral and I_2-doped tapes could be measured by directly attaching gold wires to the tape. After doping with I_2, the colour of the tape changed from purple to black, and the tape behaved as a semiconductor up to $2.6 \times 10^{-4}\,\mathrm{S\,cm^{-1}}$.

Keywords: tetrathiafulvalene; TTF; pyridine; self-assembly; nanostructure

Introduction

The synthetic chemistry of tetrathiafulvalenes (TTFs) has developed over the past 35 years (*1*), and their physical properties, such as conductivity (*2*), superconductivity (*3*) and magnetic properties (*4*), have been extensively investigated by materials scientists. However, little attention has been given to self-assembled nanostructures of TTFs, except in relation to the 'fastener effect' of TTF derivatives with long alkyl chains (*5*). In the case of redox-active TTF fibres, Jørgensen et al. (*6*) reported pioneering work in 1994, and several groups have recently reported that TTFs and their oligomers form nanostructures, such as nanofibres, nanotapes and nanotubes (*7*, *8*). In the course of our studies on multi-functional TTFs (*9*), we have been interested in long-range magnetic coupling between localised spins of organic radicals (π-electron) and transition metals (d-electron) through mobile electrons of the conducting $\pi-\pi$ networks (*10*). In order to construct molecules having strong intramolecular d–π interactions and/or charge-transfer (CT) interactions, we have designed a diad system composed of covalently linked TTF and metal–pyridine moieties (*11*). Furthermore, amphiphilic bis(pyridylethynyl)TTF **1** should form nanostructures by simply introducing a long lipophilic alkylthio chain, as shown in Figure 1 (*12*). We report here the self-assembly and nanostructured tape formation of amphiphilic TTF **1**.

Results and discussions

Bis(pyridylethynyl)TTF **1** and the related TTF **2** were synthesised using the procedure shown in Scheme 1. Phosphite-mediated coupling of 4,5-diiodo-1,3-dithiole-2-one (**3**) with 4,5-bis(dodecylthio)- (**4a**) and 4,5-bis(ethylthio)-1,3-dithiole-2-thiones (**4b**) afforded the corresponding diiodo-TTFs **5a** and **5b**, respectively (*13*). Sonogashira–Hagihara cross-coupling of **5a** and **5b** with 2-ethynylpyridine in the presence of $Pd(PPh_3)_4$, CuI and Et_3N in benzene produced **1** and **2** in 65 and 69% yields, respectively.

Although **1** and **2** are stable in the solid state, they are extremely sensitive to light in solution, probably owing to an electron-transfer reaction from the TTF core to a pyridylethynyl moiety, causing them to decompose to form a brown solid. Therefore, all experiments were carried out in the dark.

TTF-pyridine dyad **1** forms a supramolecular fibrous structure under various conditions because of its amphiphilic nature. For example, several hours after the addition of a 10-fold amount of MeOH into a red CH_2Cl_2 solution (1 mM) of **1** at 4°C, a purple fibrous material precipitated. Characterisation of the fibrous structure using optical microscopy, scanning electron microscopy (SEM) and atomic force microscopy (AFM) revealed that the material had a well-defined tape-like structure (Figure 2). The thickness, width and length of these tapes were 1–2 μm, 50–200 μm and a few mm, respectively. Under different conditions, such as THF/H_2O, CS_2/MeOH and benzene/MeOH, **1** formed similar tape-like structures. A twisted tape structure with width and thickness similar to the above-mentioned flat tape, in which the right-handed and left-handed tapes coexist, was obtained from CH_2Cl_2/MeOH (1:10, v/v) at 4°C in the presence of a trace amount of pyridine derivative (Figure 3).[1]

---

*Corresponding author. Email: iyoda@tmu.ac.jp

ISSN 1061-0278 print/ISSN 1029-0478 online

DOI: 10.1080/10610278.2010.527978
http://www.informaworld.com

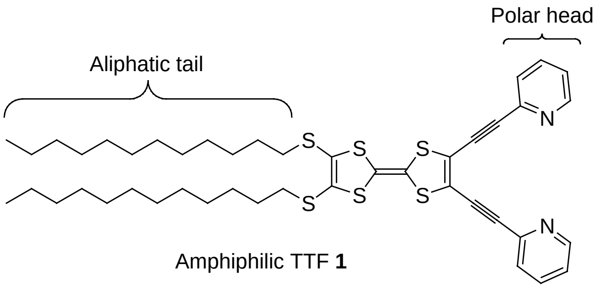

Figure 1. TTF-pyridine dyad **1**.

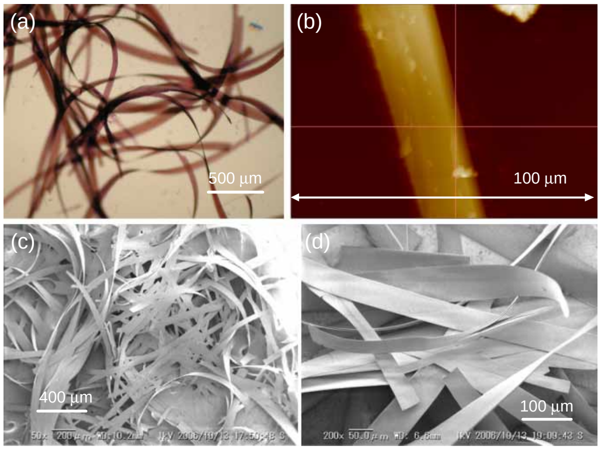

Figure 2. Microscopic images of the tape-like structure of **1** obtained from CH_2Cl_2/MeOH (1:10, v/v). (a) Optical micrograph on a glass plate, (b) AFM image on mica and (c,d) SEM image on Si wafer.

The absorption maximum of **1** at 489 nm in CH_2Cl_2 was red-shifted compared with that of 4,5-bis(butylthio)-4′,5′-bis(2-thienylethynyl)TTF (450 nm in CH_2Cl_2) (*14*) because of an intramolecular CT from the HOMO mainly located on the TTF moiety to the LUMO mainly located on the pyridine moiety. Furthermore, as shown in Figure 4, the CT absorption band of the tape (556 nm) was red-shifted in relation to the CH_2Cl_2 solution of **1** (489 nm). In addition, the colour of the CH_2Cl_2 solution was red, whereas that of the tape was purple. This suggests that the molecules aggregate in the tape structure to cause a red-shift.[2] Therefore, the relatively long-range molecular ordering may be due to intermolecular interactions between π-chromophores.

In order to obtain further information on the inner structure of the tape form of **1**, we carried out X-ray diffraction (XRD) measurements. As shown in Figure 5(a), sharp reflections were observed, indicating that the tape-like material had good crystallinity. The intense peak at $d = 43.2$ Å was assigned to the (001) reflection. In addition, higher order reflections were observed. Therefore, the tape has a lamellar structure. Although the structure of the tape is still unclear, the crystal structure of the tetrathiafulvalenohexadehydro[12]annulene derivative (*15*)[3] suggests the formation of a slipped-stack dimeric structure with a staggered cofacial arrangement with a length of 43 Å (Figure 6) (*16*). It should be noted that the XRD patterns of the tape and a drop-cast film of **1** (Figure 5(b)) are almost the same, suggesting that similar stacked structures are formed both in the tape and in the film on the surface. Although the film exhibits a sea urchin structure (a) and a striped nanotape structure (b) (Figure 7), we produced these morphologies in a short time during evaporating a CH_2Cl_2 solution of **1**. Therefore, it can be concluded that the microscale tape of **1** arises slowly from a CH_2Cl_2/MeOH (1:10, v/v) solution at 4°C.

Further information concerning the stacking of TTF-pyridine dyad could be obtained from the crystal structure of ethylthio derivative **2** (Figure 8). There were no S···S and S···H short contacts (*17*). The intermolecular CH···N interaction involving N1 and H6 (N1···H6: 2.863 Å; N1···C9: 3.628(7) Å) in **2** causes a seat structure in the b-c plane (Figure 8(a)). The TTF moiety and pyridylethynyl units in **2** form a head-to-head stacked structure along the *a*-axis (Figure 8(b)). Although the H14···H18 distance is 1.813 Å [C17···C24: 3.591(*7*) Å], which is 26% shorter than the sum of van der Waals radii (2.40 Å), the bis(pyridylethynyl) core adopts an almost planar structure.

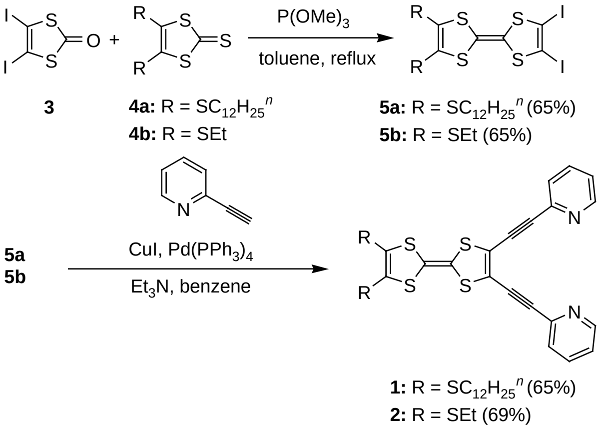

Scheme 1. Synthesis of **1** and **2**.

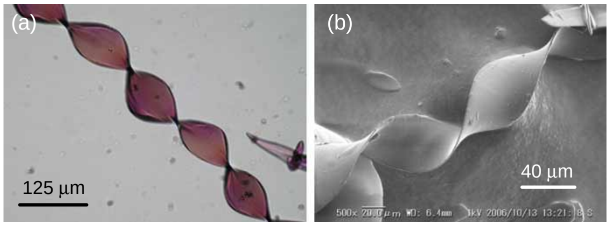

Figure 3. Microscopic images of a twisted tape of **1** obtained from CH_2Cl_2/MeOH (1:10, v/v). (a) Optical micrograph on a glass plate and (b) SEM image on Si wafer.

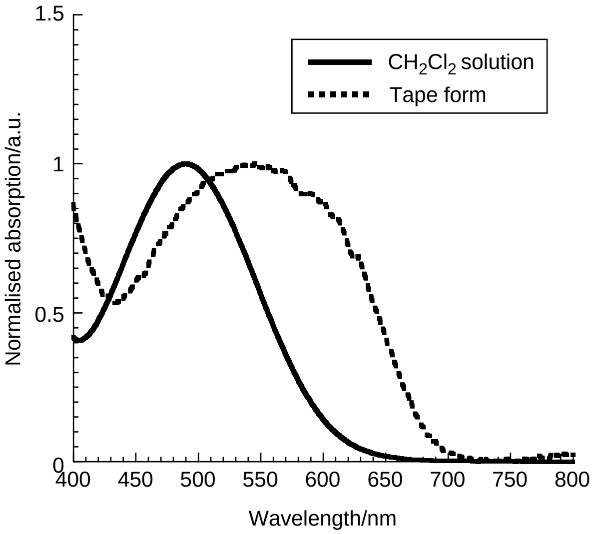

Figure 4. Electronic spectra of **1**. Solid line is for the CH_2Cl_2 solution and the dotted line is for the tape.

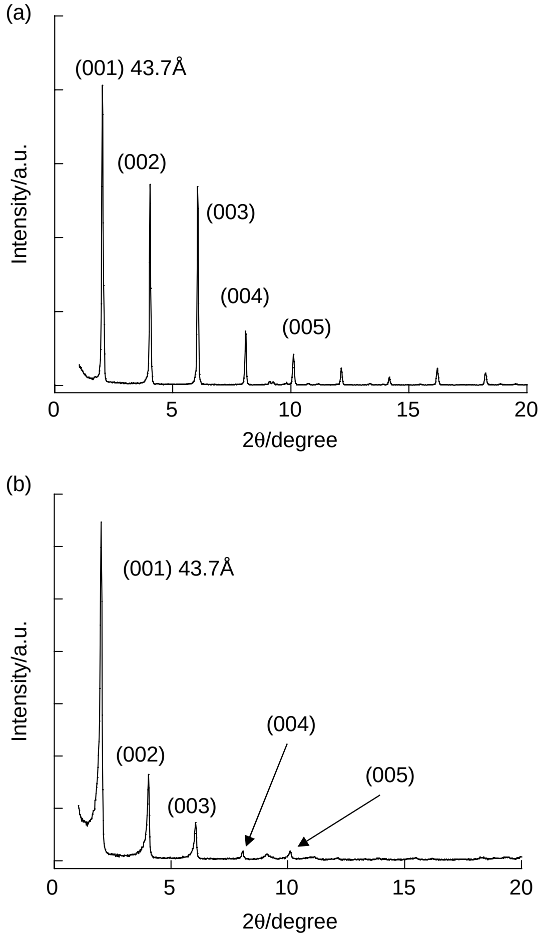

Figure 5. XRD patterns on an Al plate. (a) Tape of **1** prepared from CH_2Cl_2/MeOH. (b) Dropcast film of **1** prepared from a CH_2Cl_2 solution.

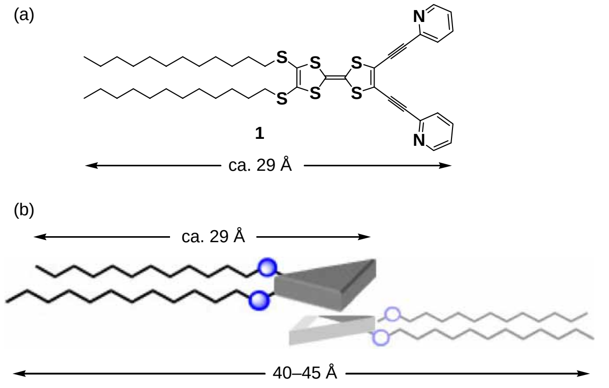

Figure 6. Proposed molecular arrangement of **1** in the tape structure. (a) Length of molecule estimated by MM2. (b) Proposed basic unit of the tape structure.

The redox properties of **1** were determined using cyclic voltammetry (CV). As shown in Figure 9, two reversible one-electron oxidations at $E_{1/2}^{\mathrm{ox1}} = 0.18\,\mathrm{V}$ and $E_{1/2}^{\mathrm{ox2}} = 0.46\,\mathrm{V}$ vs. Fc/Fc$^+$ were observed. The redox potentials of **1** are almost the same as those of both **2** and the previously reported methylthio derivative (*11*). In other words, **1** has a moderate donor ability, which is due to the two pyridylethynyl moieties.

In order to evaluate the functionality of the tape-like architecture of **1**, we measured electrical conductivities before and after being doped with iodine. A large single piece of tape was used to measure the conductivity (Figure 10). Although the neutral tape was an insulator, when the tape was doped with iodine, its conductivity increased rapidly for 8 min, and it behaved as a semiconductor with a maximum conductivity of $2.6 \times 10^{-4}\,\mathrm{S\,cm^{-1}}$ (Figure 11). After 10 min, the conductivity gradually decreased to $1.5 \times 10^{-4}\,\mathrm{S\,cm^{-1}}$ and reached a steady state.

Summary

Amphiphilic TTF **1** and the related TTF **2** were synthesised. Compound **1** formed 1D flat and helical tapes, whereas **2** formed single crystals. Tapes of **1** had a lamellar structure, and the stacked structure of **1** in the tapes was deduced in relation to the X-ray crystal structure of the corresponding methylthio derivative and **2**. Since **1**

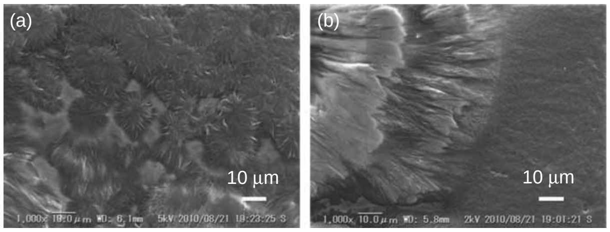

Figure 7. SEM images of a film of **1**. (a) A sea urchin structure. (b) A striped nanotape structure.

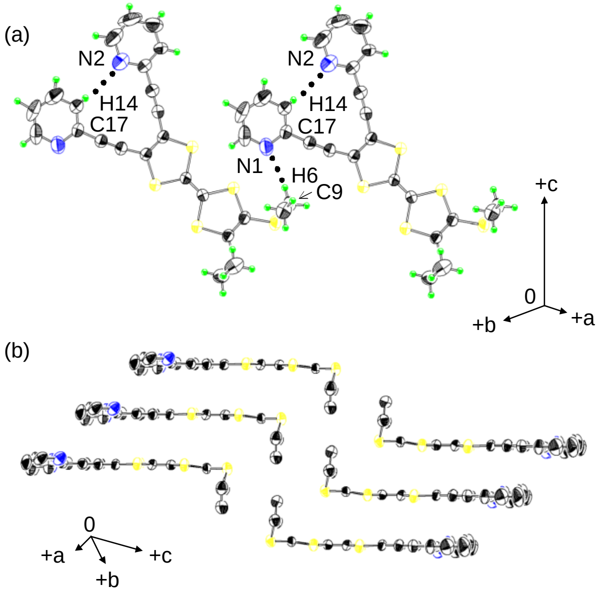

Figure 8. Packing structure of **2**. (a) Intra- and intermolecular CH···N interactions. (b) Side view. Selected interatomic distances (Å) are as follows: N1···C9 3.628(7); C17···C24 3.591(7).[4]

had fairly low oxidation potentials, its radical cation should be stable. An I_2-doped tape of **1** was semiconducting with a maximum conductivity of $2.6 \times 10^{-4}\,\mathrm{S\,cm^{-1}}$.

Experimental

Apparatus and materials

^{1}H and ^{13}C NMR spectra were recorded on a JEOL JNM-Lambda 500 or JEOL JNM-Lambda 400 spectrometer in $CDCl_3$ with Me_4Si as an internal standard unless otherwise specified. Mass spectra were recorded on a SHIMADZU GCMS-QP2010 or KRATOS AXIMA-CFR mass spectrometer. Elemental analyses were performed in the microanalysis laboratory of Tokyo Metropolitan University. Melting points were determined using a Yanaco MP-500D melting point apparatus. Electronic Spectra were recorded on a SHIMADZU UV-3101-PC spectrophotometer. CV was performed on a BAS ALS-620B electrochemical analyser. Optical images were acquired using an OLYMPUS BX-51 optical microscope. SEM images were acquired using a KEYENCE VE-8800 microscope. AFM measurements were performed using a KEYENCE Nanoscale Hybrid Microscope VN-800 in tapping mode. XRD intensity data were collected on a MAC SCIENCE M21X-SRX instrument at ambient temperature with monochromated Cu-Kα irradiation ($\lambda = 1.54056$ Å). Column chromatography was performed

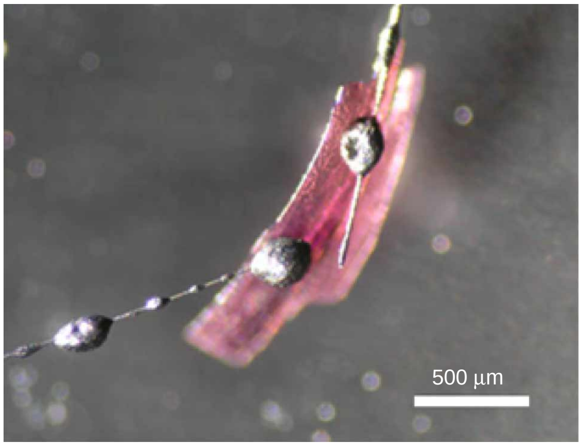

Figure 10. Optical image of tape of **1** with gold electrodes.

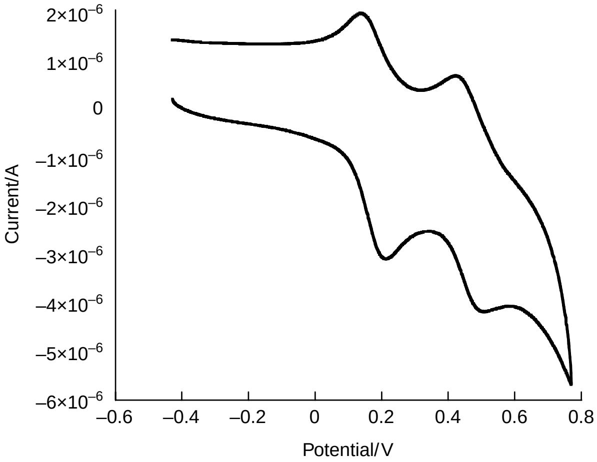

Figure 9. Cyclic voltammogram of **1**. Conditions: 0.1 M $^{n}\mathrm{Bu_4ClO_4}$ and 10^{-4} M **1** in CH_2Cl_2 at 25°C under Ar, Pt working electrode, $Ag/AgNO_3$ reference electrode, Pt wire counter electrode. Potentials are referred to $\mathrm{Fc/Fc^+}$.

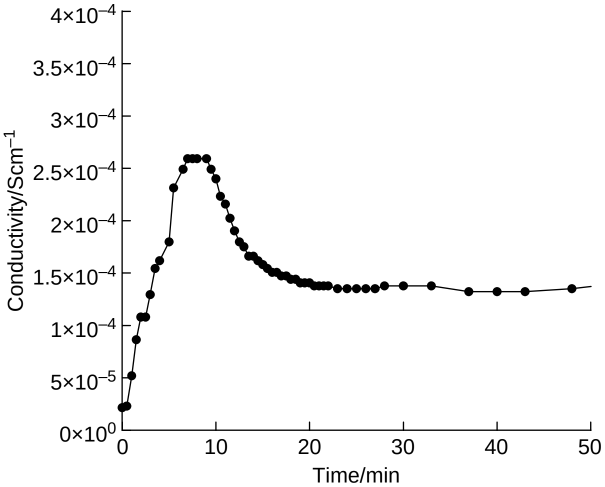

Figure 11. Electric conductivities of a single piece of tape in saturated iodine vapour at 25°C. The measurement was started simultaneously with exposure to iodine vapour.

on Merck silica gel 60, 70–230 mesh ASTM and Daiso silica gel 1001W. All solvents were dried by conventional procedures and distilled before use.

4,5-Diiodo-4′,5′-bis(dodecylthio)TTF (5a)

P(OMe)$_3$ (12.4 ml, 105 mmol) was added to a refluxing solution of **3** (1.29 g, 3.50 mmol) and **4a** (3.75 g, 7.0 mmol) in toluene (40 ml). The solution was stirred for 3 h under reflux, during which time the colour changed from yellow to dark red. The solution was concentrated *in vacuo*, and the residue was purified using column chromatography on silica gel with hexane-CS$_2$ (5:1, v/v) as the eluent. Recrystallisation from hexane gave pure **5a** (1.95 g, 2.27 mmol, 65% yield based on **3**) as a yellow solid; mp 81–82°C; EI-MS: *m/z* 856 (M$^+$); ^{1}H NMR (500 MHz, CDCl$_3$) δ (ppm) 2.80 (t, 4H, $J = 7.2$ Hz), 1.61 (quintet, 4H, $J = 7.2$ Hz), 1.39 (quintet, $J = 7.2$ Hz, 4H), 1.26 (m, 32H), 0.88 (t, 6H, $J = 7.2$ Hz); ^{13}C NMR (100 MHz, CDCl$_3$) δ (ppm) 128.1, 117.2, 111.7, 77.3, 36.8, 32.3, 30.1, 30.1, 30.1, 30.0, 29.9, 29.8, 29.5, 28.9, 23.1, 14.6; anal. calcd for $C_{30}H_{50}I_2S_6$: C, 42.05%; H, 5.88%. Found: C, 41.76%; H, 5.65%.

Synthesis of 4,5-bis(dodecylthio)-4′,5′-bis(2-pyridylethynyl)TTF (1)

4,5-Diiodo-4′,5′-bis-(dodecylthio)TTF **5a** (429 mg, 0.500 mmol), 2-ethynylpyridine (155 mg, 1.50 mmol), Pd(PPh$_3$)$_4$ (57.8 mg, 50.0 μmol), CuI (19.0 mg, 100 μmol) and Et$_3$N (0.42 ml, 3.0 mmol) in benzene (8 ml) were stirred at room temperature for 1 h under N$_2$. The reaction was quenched by the addition of water, and then the reaction mixture was extracted with CH$_2$Cl$_2$. The organic layer was dried over MgSO$_4$, and the solvent was removed under reduced pressure to give a crude product, which was chromatographed on silica gel with CH$_2$Cl$_2$–EtOAc (10:1 v/v) as the eluent. Recrystallisation from CH$_2$Cl$_2$–MeOH at 4°C afforded pure **1** (527 mg, 653 mmol, 65%) as purplish tapes; mp 89–90°C; LDI-TOF MS: *m/z* 806 (M$^+$); ^{1}H NMR (500 MHz, CDCl$_3$) δ (ppm) 8.64 (d, $J = 5.0$ Hz, 2H), 7.69 (m, 2H), 7.58 (d, $J = 7.7$ Hz, 2H), 7.28 (m, 2H), 2.82 (t, $J = 7.3$ Hz, 4H), 1.64 (quintet, $J = 7.3$ Hz, 4H), 1.41 (quintet, $J = 7.3$ Hz, 4H), 1.26 (m, 32H), 0.87 (t, $J = 7.3$ Hz, 6H); ^{13}C NMR (CDCl$_3$, 125 MHz) δ (ppm) 150.6, 142.6, 136.6, 128.3, 128.2, 123.9, 122.2, 98.5, 80.4, 78.9, 78.9, 36.8, 32.3, 30.1, 30.0, 30.0, 30.0, 29.9, 29.7, 29.5, 28.9, 23.0, 14.5; anal. calcd for $C_{44}H_{58}N_2S_6$: C, 65.46%; H, 7.24%; N, 3.47%. Found: C, 65.17%; H, 7.20%; N, 3.55%.

4,5-Diiodo-4′,5′-bis(ethylthio)TTF (5b)

When we used a synthetic procedure similar to that of **5a**, phosphite-mediated coupling of **3** (1.17 g, 3.15 mmol) and **4b** (1.60 g, 6.29 mmol) afforded **5b**. The crude product was purified using column chromatography on silica gel with hexane-CS$_2$ (1/1, v/v) as the eluent. Recrystallisation from hot hexane gave pure **5b** (1.18 g, 2.05 mmol, 65% yield based on **3**) as a yellow powder; mp 91–92°C; LDI-TOF MS: *m/z* 575 (M$^+$); ^{1}H NMR (500 MHz, CDCl$_3$) δ (ppm) 2.84 (quartet, 4H), 1.31 (s, 6H); ^{13}C NMR (100 MHz, THF-d_8) δ (ppm) 129.6, 119.6, 111.3, 79.0, 31.9, 16.3. Anal. calcd for $C_{10}H_{10}I_2S_6$. C: 20.84%, H: 1.75%; Found C: 21.17%, H: 1.82%.

Synthesis of 4,5-bis(ethylthio)-4′,5′-bis(2-pyridylethynyl)TTF (2)

When we used a synthetic procedure similar to that of **1**, Sonogashira–Hagihara coupling of 4,5-diiodo-4′,5′-bis-(ethylthio)TTF **5b** (239.3 mg, 0.415 mmol) with 2-ethynylpyridine (129 mg, 1.25 mmol) afforded **2**. Recrystallisation from hot hexane afforded pure **2** (150.8 mg, 0.286 mmol, 69% yield) as dark red needles; mp 86–88°C; EI-MS: *m/z* 526 (M$^+$); ^{1}H NMR (CDCl$_3$, 500 MHz) δ (ppm) 8.63 (d, $J = 4.9$ Hz, 2H), 7.69 (m, 2H), 7.58 (d, $J = 7.7$ Hz, 2H), 7.27 (m, 2H), 2.86 (quartet, $J = 7.3$ Hz, 4H), 1.32 (t, $J = 7.3$ Hz, 6H); ^{13}C NMR (125 MHz, CDCl$_3$) δ (ppm) 150.2, 142.2, 136.2, 127.8, 127.6, 123.5, 121.8, 112.4, 109.8, 98.2, 79.9, 19.3; anal. calcd for $C_{24}H_{18}N_2S_6$: C, 54.72%; H, 3.44%; N, 5.32%. Found: C, 54.87%; H, 3.45%; N, 5.46%.

X-ray analysis for 2

X-ray analysis was performed on a Bruker AXS SMART APEX CCD diffractometer at 293 K with graphite-monochromated Mo-Kα radiation ($\lambda = 0.71073$ Å). $C_{24}H_{18}N_2S_6$, MW = 526.8, triclinic, $P-1$ (#2), $Z = 2$, $a = 5.4140(6)$ Å, $b = 9.8887(10)$ Å, $c = 23.585(2)$ Å, $\alpha = 96.145(2)°$, $\beta = 96.071(2)°$, $\gamma = 92.871(2)°$, $V = 1246.0(2)$ Å^3, $D_{\mathrm{calcd}} = 1.404$ g/cm^3, $T = 278$ K, $R_1 = 0.043$, $R_{\mathrm{w}} = 0.143$, goodness-of-fit = 1.108. A total of 5660 reflections with 3588 being unique were observed, and 2463 reflections ($I > 2.00\sigma(I)$) were used for the refinement (340 parameters). The crystal structure was solved using SHELXS-97 and refined by using the full matrix least-squares method included in SHELXL-97. Cambridge Crystallographic Data Centre deposition No. CCDC–790401. Unfortunately, unlike the structures of other pyridine derivatives, in which the C—C and C═N bonds were definitely assigned, the alignment of pyridine rings in **2** was not exactly determined due to their large temperature factors. Considering the interaction and steric repulsion with adjacent molecules and the structure of methyl derivative (*11*), the most reasonable structure is shown in Figure 8.

Acknowledgements

This work was partially supported by a grant-in aid for Scientific Research from the Ministry of Education, Culture, Sports, Science and Technology of Japan. The authors are greatly indebted to Dr Masashi Hasegawa (Kitasato University), Dr Hideo Enozawa (RIKEN) and Mr Ken-ichi Tokuyama (Tokyo Metropolitan University) for helpful discussions.

Notes

1. A trace amount of amines such as Et_3N, Et_2NH and $(i\text{-}Pr)_2NH$ causes a twisted structure.
2. Although the electronic spectra of **1** and **2**, and the related methylthio derivative (*11*) in CH_2Cl_2 solution exhibited the absorption maxima at 486–489 nm, the tape of **1** showed a marked red-shift of the absorption maximum at 556 nm, presumably owing to a strong stacking. In contrast, the films of **2** exhibited the absorption maximum at 502 nm, reflecting rather random stacking.
3. Dibenzotetrathiafulvalenohexadehydro[12]annulene forms a slipped-stack dimer with a staggered cofacial arrangement like the dimer of **1** in Figure 6.
4. Although the XRD profile of the microscale tape of **1** shows a simple lamellar structure (Figure 5(a)), the XRD profile of single crystals of **2** is very complex owing to its 3D network structure.

References

(1) (a) Yamada, J.; Sugimoto, T., Eds. *TTF Chemistry*; Kodansha & Springer-Verlag: Tokyo, 2004. (b) Yamada, J.; Akutsu, H.; Nishikawa, H.; Kikuchi, K. *Chem. Rev.* **2004**, *104*, 5057–5084. (c) Iyoda, M.; Hasegawa, M.; Miyake, Y. *Chem. Rev.* **2004**, *104*, 5085–5114. (d) Jeppesen, J.O.; Nielsen, M.B.; Becher, J. *Chem. Rev.* **2004**, *104*, 5115–5132. (e) Fabre, J.M. *Chem. Rev.* **2004**, *104*, 5133–5150.

(2) (a) Geiser, U.; Schlueter, J.A. *Chem. Rev.* **2004**, *104*, 5203–5242. (b) Fourmigué, M.; Batail, P. *Chem. Rev.* **2004**, *104*, 5379–5418. Papavassiliou, G.C.; Terzis, A.; Delhaes, P. In *Handbook of Organic Conductive Molecules and Polymers*; Nalwa, H.S., Ed.; John Wiley & Sons: Chichester, 1997; pp 151–227.

(3) (a) Kobayashi, H.; Cui, H.; Kobayashi, A. *Chem. Rev.* **2004**, *104*, 5265–5288. (b) Shibaeva, R.P.; Yagubskii, E.B. *Chem. Rev.* **2004**, *104*, 5347–5378. (c) Jérome, D. *Chem. Rev.* **2004**, *104*, 5565–5592.

(4) (a) Coronado, E.; Day, P. *Chem. Rev.* **2004**, *104*, 5419–5448. (b) Enoki, T.; Miyazaki, A. *Chem. Rev.* **2004**, *104*, 5449–5478.

(5) Inokuchi, H.; Saito, G.; Wu, P.; Seki, K.; Tang, T.B.; Mori, T.; Imaeda, K.; Enoki, T.; Higuchi, Y. *Chem. Lett.* **1986**, *15*, 1263–1266.

(6) Jørgensen, M.; Bechgaard, K.; Bjørnholm, T.; Sommer-Larsen, P.; Hansen, L.G.; Schaumburg, K. *J. Org. Chem.* **1994**, *59*, 5877–5882.

(7) (a) Sly, J.; Kasák, P.; Gomar-Nadal, E.; Rovira, C.; Górriz, L.; Thorarson, P.; Amabilino, D.B.; Rowan, A.E.; Nolte, R.J.M. *Chem. Commun.* **2005**, 1255–1257. (b) Akutagawa, T.; Kakiuchi, K.; Hasegawa, T.; Noro, S.; Nakamura, T.; Hasegawa, H.; Mashiko, S.; Becher, J. *Angew. Chem. Int. Ed.* **2005**, *44*, 7283–7287. (c) Kitamura, T.; Nakaso, S.; Mizoshita, N.; Tochigi, Y.; Shimomura, T.; Moriyama, M.; Ito, K.; Kato, T. *J. Am. Chem. Soc.* **2005**, *127*, 14769–14775. (d) Kitahara, T.; Shirakawa, M.; Kawano, S.; Beginn, U.; Fujita, N.; Shinkai, S. *J. Am. Chem. Soc.* **2005**, *127*, 14980–14981. (e) Wang, C.; Zhang, D.; Zhu, D. *J. Am. Chem. Soc.* **2005**, *127*, 16372–16373.

(8) (a) Iyoda, M.; Hasegawa, M.; Enozawa, H. *Chem. Lett.* **2007**, *36*, 1402–1407. (b) Hasegawa, M.; Enozawa, H.; Iyoda, M. *J. Synth. Org. Chem.* **2008**, *66*, 1211–1222. (c) Hasegawa, M.; Iyoda, M. *Chem. Soc. Rev.* **2010**, *39*, 2420–2427.

(9) (a) Honna, Y.; Isomura, E.; Enozawa, H.; Hasegawa, M.; Takase, M.; Nishinaga, T.; Iyoda, M. *Tetrahedron Lett.* **2010**, *51*, 679–682. (b) Hara, K.; Hasegawa, M.; Kuwatani, Y.; Enozawa, H.; Iyoda, M. *Heterocycles* **2010**, *80*, 909–915. (c) Hasegawa, M.; Kobayashi, Y.; Hara, K.; Enozawa, H.; Iyoda, M. *Heterocycles* **2009**, *77*, 837–842. (d) Enozawa, H.; Hasegawa, M.; Isomura, E.; Nishinaga, T.; Kato, T.; Yamato, M.; Kimura, T.; Iyoda, M. *Chem PhysChem* **2009**, *10*, 2607–2611. (f) Hasegawa, M.; Enozawa, H.; Kawabata, Y.; Iyoda, M. *J. Am. Chem. Soc.* **2007**, *129*, 3072–3073. (g) Enozawa, H.; Hasegawa, M.; Takamatsu, D.; Fukui, K.; Iyoda, M. *Org. Lett.* **2006**, *8*, 1917–1920. (h) Iyoda, M.; Enozawa, H.; Miyake, Y. *Chem. Lett.* **2004**, *33*, 1098–1099. (i) Iyoda, M.; Hara, K.; Ogura, E.; Takano, T.; Hasegawa, M.; Yoshida, M.; Kuwatani, Y.; Nishikawa, H.; Kikuchi, K.; Ikemoto, I.; Mori T. *J. Solid State Chem.* **2002**, *168*, 597–607. (j) Iyoda, M.; Hasegawa, M.; Takano, J.; Hara, K.; Kuwatani, Y. *Chem. Lett.* **2002**, *31*, 590–591. (k) Iyoda, M.; Hasegawa, M.; Kuwatani, Y.; Nishikawa, H.; Fukami, K.; Nagase, S.; Yamamoto, G. *Chem. Lett.* **2001**, *30*, 1146–1147. (l) Iyoda, M.; Hara, K.; Kuwatani, Y.; Nagase, S. *Org. Lett.* **2000**, *2*, 2217–2220.

(10) (a) Nishijo, J.; Ogura, E.; Yamaura, J.; Miyazaki, A.; Enoki, T.; Takano, T.; Kuwatani, Y.; Iyoda, M. *Solid State Commun.* **2000**, *116*, 661–664. (b) Iyoda, M.; Takano, T.; Otani, N.; Ugawa, K.; Yoshida, M.; Matsuyama, H.; Kuwatani, Y. *Chem. Lett.* **2001**, *30*, 1310–1311. (c) Miyazaki, A.; Enomoto, K.; Okabe, K.; Yamazaki, H.; Nishijo, J.; Enoki, T.; Ogura, E.; Ugawa, K.; Kuwatani, Y.; Iyoda, M. *Solid State Commun.* **2002**, *168*, 547–562.

(11) Isomura, E.; Tokuyama, K.; Nishinaga, T.; Iyoda, M. *Tetrahedron Lett.* **2007**, *48*, 5895–5898.

(12) For examples, see: (a) Kobayashi, Y.; Hasegawa, M.; Enozawa, H.; Iyoda, M. *Chem. Lett.* **2007**, *36*, 720–721. (b) Enozawa, H.; Honna, Y.; Iyoda, M. *Chem. Lett.* **2007**, *36*, 1434–1435.

(13) (a) Iyoda, M.; Kuwatani, Y.; Hara, K.; Ogura, E.; Suzuki, H.; Ito, H.; Mori, T. *Chem. Lett.* **1997**, *26*, 599–600. (b) Kuwatani, Y.; Ogura, E., Nishikawa, H.; Ikemoto, I.; Iyoda, M. *Chem. Lett.* **1997**, *26*, 817–818.

(14) Hasegawa, M.; Hara, K.; Tokuyama, K.; Iyoda, M. *Phosphorous Sulfur Silicon* **2010**, *185*, 1061–1067.

(15) Hara, K.; Hasegawa, M.; Kuwatani, Y.; Enozawa, H.; Iyoda, M. *Chem. Commun.* **2004**, 2042–2043.

(16) The bis(pyridylethynyl)TTF moiety in **1** may stack in a slipped geometry, and the dodecylthio groups may adopt a bent structure. Therefore, the basic unit of the tape structure (Figure 6(b)) was estimated a little smaller than the MM2 structure (Figure 6(a)), see: Saito, G.; Yoshida, Y. *Bull. Chem. Soc. Jpn* **2007**, *80*, 1–137.

(17) For example, see: Hasegawa, M.; Takano, J.; Enozawa, H.; Kuwatani, Y.; Iyoda, M. *Tetrahedron Lett.* **2004**, *45*, 4109–4112.